

A Simple Analysis For **GAS SEPARATION MEMBRANE EXPERIMENTS**

RICHARD A. DAVIS, ORVILLE C. SANDALL*
University of Minnesota Duluth • Duluth, MN 55812

Membrane applications for gas separations have made rapid advances over the past decade.^[1] In some cases, membrane technologies have been used to enhance or replace more traditional methods of gas purification. The need for educating undergraduate chemical engineering students about membrane-based separations has not gone unnoticed. Newer editions of popular separations textbooks have added chapters on membranes with sections on gas permeation.^[2-4]

Earlier, Davis and Sandall^[5] described an undergraduate laboratory membrane experiment and analysis for separating the components of air. It remains relevant today as one approach to providing students with hands-on experience with this important technology. The experimental objectives included an inverse mass transfer analysis of experimental data for key membrane transport parameters. The original analysis involved solving a set of differential species balances and fitting the results to experimental data by iterative, trial-and-error techniques. They found that the numerical methods required to implement their analysis were beyond the scope of the undergraduate chemical engineering laboratory experience. Consequently, they provided students with True BASIC programs that were used to solve the model equations. Unfortunately, the programs were limited to the specific membrane configuration in the laboratory. Students were unable to explore alternative designs using the validated models without modifying the programs. In the meantime, several popular, modern, computational software applications (such as Excel, Mathcad, Matlab, or Polymath) have emerged that provide readily accessible tools for solving complex problems that involve nonlinear algebraic and differential equations. The drawbacks in the original analysis, along with developments in computational tools, have led to a simpler alternative analysis described in this paper.

EXPERIMENT

Davis and Sandall^[5] provided specific details of the experimental objectives, apparatus, and procedure for a commercial hollow-fiber membrane unit for air separation. The Prism separator developed by Permea

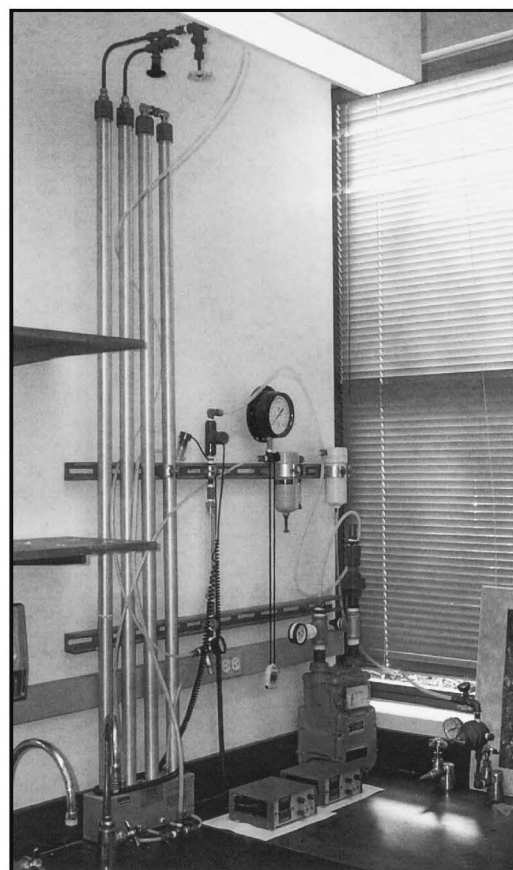


Figure 1. Prism hollow-fiber membrane apparatus.

Richard A. Davis is Associate Professor in the Department of Chemical Engineering at the University of Minnesota Duluth. He earned his BS in Chemical Engineering from Brigham Young University and his PhD from the University of California, Santa Barbara. He teaches a variety of courses in transport phenomena and separations, and his current research interests include process modeling and optimization.

Orville C. Sandall is Professor of Chemical Engineering at the University of California, Santa Barbara. He is a graduate of the University of Alberta (BSc and MSc) and the University of California, Berkeley (PhD). His teaching and research interests are in the areas of mass transfer and separation processes.

* University of California, Santa Barbara, CA 93106

Membranes in ChE Education

Corporation, shown in Figure 1, consists of four hollow-fiber membrane modules arranged in a series of columns. Each module is a shell-and-tube arrangement of a bundle of hollow-fiber membranes that are capped at the top. High-pressure feed air is introduced to the shell side of the fibers. The permeating gas flows through the hollow-fiber bores and is collected in a manifold at the open end. The pressure drop across the shell side of the membrane unit was found to be negligible.^[5] The permeate streams are open to the atmosphere. The pressure at the closed end of the fiber bores is not directly measurable in the current module arrangements. Information about fiber length, fiber inside diameter, and the number of fibers in the Prism separator bundle is not available, but a conservative estimate of the pressure build-up in the fiber bore was calculated to increase by less than nine percent above atmospheric pressure for the range of experimental operating conditions. For most of the experiments, the pressure build-up was estimated to be less than three percent.

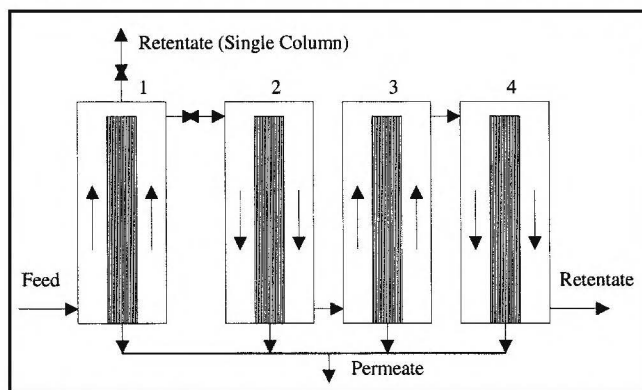


Figure 2. Schematic of single, countercurrent flow column or four columns with alternating flow patterns.

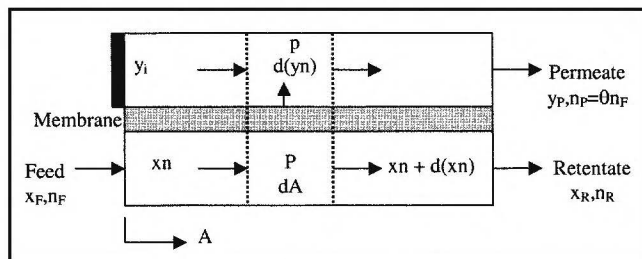


Figure 3. Ideal cocurrent flow pattern

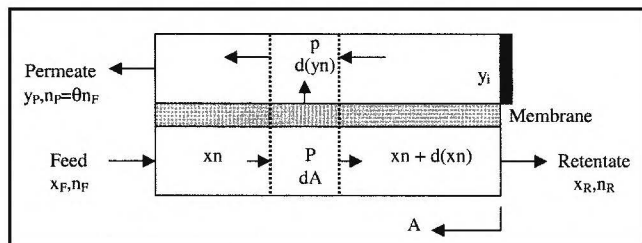


Figure 4. Ideal countercurrent flow pattern.

Modern gas-separation membrane modules introduce the high-pressure feed to the bore side of the fibers to eliminate channeling and maintain a more uniform flow distribution. High-pressure feed to the fiber bores can result in a significant axial pressure drop in the fibers. Although not required for this membrane module, the effects of pressure are included in the analysis for completeness.

As shown in the schematic of Figure 2, the air-flow pattern consists of alternating countercurrent and cocurrent flow through the columns. The composition of the retentate and permeate streams was measured with oxygen analyzers. The flow rate of the retentate stream was measured with a volumetric flow meter. The feed and permeate flow rates may be calculated by mass balances.

The membrane separator may be operated as four columns in series, or as a single column by closing a valve on the tube connecting the retentate and feed streams between the first two columns. The first column operates in countercurrent flow and was used to calibrate the membrane models from a series of runs performed at various feed-flow rates and pressures. The calibrated model was confirmed by favorable comparisons of model predictions with experimental results from the four-column configuration.

THEORY AND ANALYSIS

A differential model of binary gas separation in the membrane experiment was validated by Davis and Sandall and is summarized next. For the conditions of the experiment, it can be shown that a simplification to the equations permits an algebraic solution.

The mathematical model of membrane gas separation was based on several key assumptions. First, the temperature was assumed to be constant. Further, it was assumed that all streams through the shell and permeate sides of the fibers were in plug flow. The air fed to the unit was assumed to be a binary mixture of 79% N_2 and 21% O_2 . All four columns were assumed to have the same dimensions and specific area for mass transfer. Finally, axial pressure drop was ignored for the fiber bore. This assumption is valid for low permeate flow or large transmembrane pressure differences where small changes in permeate pressure are negligible relative to the high feed pressure.

■ Differential Model

Walawender and Stern^[6] derived the differential equations for a binary gas system in countercurrent and cocurrent plug flow patterns, shown ideally in Figures 3 and 4. Details of the derivation are available in several references.^[3,5,6] For a binary gas system, the total mole and O_2 species balances around the separator are

Membranes in ChE Education

$$n_F = n_R + n_p \quad (1)$$

$$x_F n_F = x_R n_R + y_p n_p \quad (2)$$

where n_F , n_R , and n_p are the molar flow rates of the feed, retentate, and permeate streams, respectively, and x_F , x_R , and x_p are the feed, retentate, and permeate O_2 mole fractions, respectively. The species balances around a differential volume element in the membrane give

$$d(xn) = Q_{O_2}'(xP - yp)dA \quad (3)$$

$$d[(1-x)n] = Q_{N_2}'[(1-x)P - (1-y)p]dA \quad (4)$$

where Q_j' is the permeance of species j , A is the membrane surface area, and P and p are the average retentate and permeate side pressures, respectively.

For convenience in the analysis, Eqs. (1) to (4) were combined into the following dimensionless equations for countercurrent flow:

$$K_R \frac{dx}{dA^*} = \left(\frac{x-y}{x_R - y_i} \right) \left\{ \alpha^* (1-x)(xr-y) - x[(1-x)r - (1-y)] \right\} \quad (5)$$

$$K_R \frac{dy}{dA^*} = \left(\frac{x-y}{x_R - x} \right) \left\{ \alpha^* (1-y)(xr-y) - y[(1-x)r - (1-y)] \right\} \quad (6)$$

$$K_R \frac{dn^*}{dA^*} = \alpha^* (xr-y) + (1-x)r - (1-y) \quad (7)$$

where y_i is the mole fraction in the permeate at the closed end of the fibers. The dimensionless transport parameters are defined as

$$A^* = A / A_m \quad (8)$$

$$r = P / p \quad (9)$$

$$K_R = n_R / Q_{N_2}' A_m P \quad (10)$$

$$\alpha^* = Q_{O_2}' / Q_{N_2}' \quad (11)$$

$$n^* = n / n_R \quad (12)$$

where A_m is the total membrane area. The ideal separation factor, α^* , was assumed constant, but the dimensionless transport parameter, K_R , was defined as a function of the retentate molar flow rate. The solution to Eq. (7) was used to check the assumptions leading to the algebraic model of the next section. The countercurrent flow equations are integrated from the retentate end of the membrane, subject to the initial conditions

$$\left. \begin{array}{l} x = x_R \\ y = y_i \\ n^* = 1 \end{array} \right\} \text{at } A^* = 0 \quad (13)$$

Note the discontinuity in Eq. (6) at $x = x_R$ requires application of l'Hôpital's rule.^[6]

The dimensionless cocurrent flow model equations are

$$K_F \frac{dx}{dA^*} = \left(\frac{x-y}{y - x_F} \right) \left\{ \alpha^* (1-x)(xr-y) - x[(1-x)r - (1-y)] \right\} \quad (14)$$

$$K_F \frac{dy}{dA^*} = \left(\frac{x-y}{x - x_F} \right) \left\{ \alpha^* (1-y)(xr-y) - y[(1-x)r - (1-y)] \right\} \quad (15)$$

where

$$K_F = \frac{n_F}{Q_{N_2}' A_m P} \quad (16)$$

The cocurrent model equations are integrated from the feed end, subject to the initial conditions

$$\left. \begin{array}{l} x = x_F \\ y = y_i \end{array} \right\} \text{at } A^* = 0 \quad (17)$$

The permeate composition at the capped end of the hollow fibers is calculated from the ratio of Eqs. (3) and (4)

$$\frac{y_i}{1-y_i} = \frac{\alpha^* [xr - y_i]}{[(1-x)r - (1-y_i)]} \quad (18)$$

where, for countercurrent flow, $x = x_R$. For cocurrent flow, $x = x_F$. Equation (18) is quadratic in y_i . Note that there is an error in the denominators of Eqs. (17) and (22) of the paper by Davis and Sandall.^[5] The correct solution to the quadratic equation is

$$y_i = \frac{(\alpha^* - 1)(xr+1) + r - \sqrt{[(\alpha^* - 1)(xr+1) + r]^2 - 4(\alpha^* - 1)\alpha^* xr}}{2(\alpha^* - 1)} \quad (19)$$

Davis and Sandall successfully used the differential model in their analysis of O_2/N_2 separation in the membrane module. At the time, they found that the background required to solve the model equations for α^* and K_R was beyond the scope of an undergraduate student in their laboratory course. Consequently, they developed True BASIC programs that were provided to the students to solve the model equations. Since then, advances in computational software (such as Mathcad) have simplified the process of solving the model

equations. Undergraduate students are now able to develop their own solutions using standard numerical methods for solving systems of nonlinear equations or differential equations that are readily available in these computer tools.

Nevertheless, students are still required to set up a standard method such as Euler's or Runge-Kutta for the initial-value problems in order to find the values for α^* and K_R by inverse analysis of the first column in countercurrent flow. For example, Mathcad and Polymath do not permit their intrinsic capabilities for solving systems of first-order differential equations to be treated as part of another function. An example of programming required in Mathcad for the inverse mass transfer is shown in Figure 5. This type of solution may be intimidating for undergraduate students, depending on their level of experience. This realization, along with the observation that the composition profiles along the membrane were approximately linear, led to the following alternative analysis that avoids the initial-value problem solution requirements entirely.

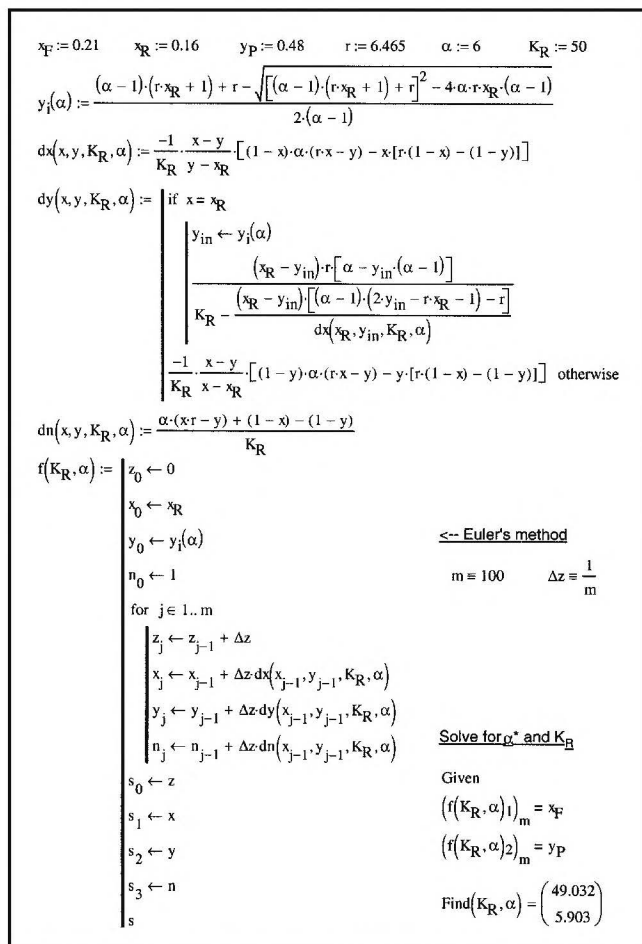


Figure 5. Example of Mathcad programming for inverse mass transfer analysis for α^* and K_R .

Algebraic Model

Boucif, *et al.*,^[7] presented a series solution to the binary component differential model Eqs. (5), (6), (14), and (15) that requires a numerical solution to a pair of third-order polynomial equations. The solution to the series equations agrees with numerical solutions to the differential model when the cut is less than 50%. The series solution does not include axial pressure effects in the feed or permeate gas, however. Hundyil and Koros^[8] presented a more complete analysis of hollow-fiber membrane modules for multicomponent gas separation that includes pressure effects. Their approach is based on a finite-volume element model that requires iterative solutions to a large system of nonlinear algebraic equations. The finite-element approach is recommended when detailed information of pressure, temperature, and composition effects is required.

A simpler, alternative analysis of the membrane unit described here was developed that involves only the solution to a small system of nonlinear algebraic equations and includes pressure effects when necessary. The simpler-model equations are analogous to the shell-and-tube heat-exchanger design equations that are familiar to undergraduate chemical engineering students. The following analysis assumes laminar flow and constant species permeances that are independent of the pressure and composition of the feed or permeate gas. The Hagen-Poiseuille equation is commonly used to calculate axial pressure effects^[9]

$$\frac{dp}{dz} = \frac{128 RT \mu n}{p \pi d_f^4 N_f} \quad (20)$$

where R is the ideal gas constant, T is the gas temperature, μ is the gas viscosity, n is the variable molar flow rate of permeate gas, d_f is the inside fiber bore diameter, and N_f is the number of fibers in a bundle. Other expressions derived from the Hagen-Poiseuille equation have been developed to account for compressibility and flow in porous channels when necessary.^[8,10-12]

It has been observed that when the change in the feed mole fraction of oxygen is less than 50%, the differential balances may be replaced with algebraic expressions involving the logarithmic mean of the transmembrane partial-pressure difference.^[13] In Eq. (3), let

$$\Delta = x_P - y_P \quad (21)$$

The driving force for diffusion across the membrane, Δ , is assumed to be a linear function of the change in the molar flow on the feed side of the membrane

$$\frac{d(xn)}{d\Delta} = \frac{(xn)_R - (xn)_F}{\Delta_R - \Delta_F} \quad (22)$$

Combine eqs. (2), (3), and (22), separate variables and inte-

Membranes in ChE Education

grate

$$y_p n_p \int_{\Delta_F}^{\Delta_R} \frac{d\Delta}{\Delta} = Q_{O_2} (\Delta_R - \Delta_F) \int_0^A dA \quad (23)$$

or

$$y_p n_p = Q_{O_2} (xP - yP)_{lm} A_m \quad (24)$$

where the log-mean difference in O_2 partial pressure across the membrane is defined as

$$(xP - yP)_{lm} = \frac{(xP - yP)_R - (xP - yP)_F}{\ln[(xP - yP)_R / (xP - yP)_F]} \quad (25)$$

A similar result is found for a N_2 flux expression

$$(1 - y_p) n_p = Q_{N_2} [(1 - x)P - (1 - y)P]_{lm} A_m \quad (26)$$

The steady-state binary-gas membrane equations can be written in dimensionless form using the average pressures

$$x_F = x_R(1 - \theta) + y_p \theta \quad (27)$$

$$y_p K_R \theta = (1 - \theta) \alpha^* (x_r - y)_{lm} \quad (28)$$

$$(1 - y_p) K_R \theta = (1 - \theta) [(1 - x)r - (1 - y)]_{lm} \quad (29)$$

where the cut is defined here as the ratio of permeate-to-feed flow rates

$$\theta = n_p / n_f \quad (30)$$

Alternative forms of Eqs. (28) and (29) in terms of K_F are

$$y_p K_F \theta = \alpha^* (x_r - y)_{lm} \quad (31)$$

$$(1 - y_p) K_F \theta = [(1 - x)r - (1 - y)]_{lm} \quad (32)$$

The permeate composition at the closed end of the hollow-fiber membranes is calculated from Eq. (19).

The experimental separation factor was calculated from the measured compositions of the permeate and retentate streams

$$\alpha = \frac{y_p(1 - x_R)}{x_R(1 - y_p)} \quad (33)$$

Under conditions where the change in the feed composition exceeds 50%, the log-mean model can be applied two or more times as necessary across a module such that each cut does not exceed a 50% change in x_F from the previous step. The pressure at the closed end of the fiber bore can be calculated by assuming that the permeate flow rate is a linear function of distance along the fiber

$$n = \frac{n_p z}{L} \quad (34)$$

where L is the fiber length. Equation (20) can be integrated with substitution from Eq. (34) to give an estimate for the permeate pressure at the closed end of the fibers^[9]

$$P_c = \sqrt{P^2 + \frac{128 RT \mu L n_p}{\pi d_f^4 N_f}} \quad (35)$$

■ Solution Method

The algebraic model Eqs. (19) and (27-29) represent a system with four degrees of freedom, or four equations in eight variables: x_F , x_R , y_p , y_r , θ , α^* , K_R , and r . The model was initially calibrated by fixing x_F and r and measuring x_R and y_p , leaving y_r , θ , α^* , and K_R as unknowns in the solution.

The solution of the system of nonlinear algebraic equations requires an iterative, trial-and-error technique, such as Newton's method. The log-mean approximation of the partial-pressure driving force is notoriously difficult to converge under these circumstances. Fortunately, there are good approximations to the log-mean that avoid problems of divergence in the solution. The following form of the Chen approximation was used:^[14]

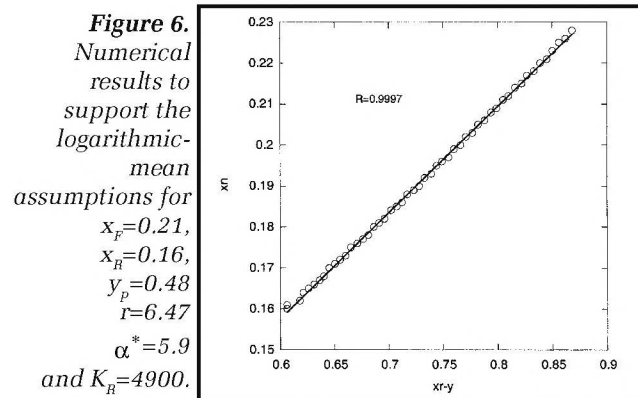
$$\frac{\Delta_2 - \Delta_1}{\ln(\Delta_2 / \Delta_1)} \cong \left[\Delta_1 \Delta_2 \frac{(\Delta_1 + \Delta_2)}{2} \right]^{1/3} \quad (36)$$

Floudas noted that the Chen approximation to the log-mean has the advantage that it becomes zero if either the feed or exit partial-pressure driving forces become zero.^[15]

The four-column configuration requires sequential solution to the countercurrent and cocurrent models. Note that $n_{2F} = n_{1R}$ and $K_{2F} = K_{1R}$ between the first and second columns, and that $n_{4F} = n_{3R}$ and $K_{4F} = K_{3R}$ between the third and fourth columns. The feed flow rates to each column are calculated from the cut for the previous column.

RESULTS AND DISCUSSION

The experimental data of Davis and Sandall^[5] were used to illustrate the analysis procedure. The assumption of Eq. (22) for the log-mean approximation was evaluated by plotting a representative numerical solution to Eq. (7), shown in Figure 6. A linear least-squares regression of the numerical results



Membranes in ChE Education

shows that the assumption of a linear function for Δ is valid for the conditions of this laboratory experiment.

A sample calculation of the single countercurrent flow model calibration using Mathcad is shown in Figure 7. The experimental data and results of the algebraic model are compared with the results from the differential model in Table 1 for α^* and K_R . There are no significant differences in the results between these models.

```

x_F := 0.21  x_R := 0.16  y_P := 0.48  r := 6.465
K_R := 50  alpha := 6  y_i := 0.5  theta := 0.2

Delta_lm(Delta_1, Delta_2) := (Delta_1 * Delta_2 * (Delta_1 + Delta_2) / 2)^(1/3)

Given

x_F = x_R * (1 - theta) + y_P * theta

y_i / (1 - y_i) = alpha * (x_R * r - y_i) / ((1 - x_R) * r - (1 - y_i))

y_P * K_R * theta = (1 - theta) * alpha * Delta_lm(x_F * r - y_P, x_R * r - y_i)

(1 - y_P) * K_R * theta = (1 - theta) * alpha * Delta_lm((1 - x_F) * r - (1 - y_P), (1 - x_R) * r - (1 - y_i))

Find(K_R, alpha, y_i, theta) = (49.024, 5.931, 0.426, 0.156)
    
```

Figure 7. Example of Mathcad calculation for inverse mass transfer analysis using the log-mean model.

TABLE 1							
Calibration Data^[5] and Results for Single Countercurrent Column							
<u>Experimental Data</u>				<u>Differential Model</u>		<u>Algebraic Model</u>	
P (kPa)	n _r × 10 ² (gmol/s)	x _R	y _P	α*	K _R	α*	K _R
377	0.73	0.18	0.43	5.81	31.1	5.82	31.1
377	0.74	0.18	0.43	5.81	31.1	5.82	31.1
377	1.03	0.19	0.44	5.98	49.6	5.98	49.6
377	1.32	0.19	0.44	5.98	49.6	5.98	49.6
377	2.54	0.20	0.44	5.71	98.7	5.71	98.6
515	0.62	0.15	0.45	5.93	26.2	5.97	26.1
515	0.73	0.16	0.46	6.02	33.3	6.05	33.2
515	0.95	0.17	0.47	6.12	43.9	6.14	43.9
515	1.51	0.18	0.47	5.85	58.2	5.86	58.2
515	2.25	0.19	0.48	5.96	92.1	5.96	92.1
653	0.74	0.14	0.46	5.78	31.5	5.84	31.4
653	0.95	0.15	0.47	5.84	38.8	5.88	38.7
653	1.32	0.16	0.48	5.90	49.1	5.93	49.0
653	2.18	0.18	0.49	5.73	85.7	5.74	85.6
653	3.44	0.19	0.5	5.81	135	5.81	135
<i>Average</i>				5.88		5.90	

A linear relationship between the retentate flow rate and K_R is calculated for use in the remaining three column predictions. The linear function is plotted with the results in Figure 5. The result of a linear least-squares regression gives

$$K_R = 4.0 \times 10^3 n_R \quad (37)$$

The average value of α^* was calculated to be 5.9 assuming atmospheric pressure in the fiber bore. An increase in fiber-bore pressure would cause the experimentally determined species permeances to decrease. The axial pressure drop has been found to vary linearly with flow rate, however.^[16] Thus, the slope in Eq. (37) is not affected by the small pressure build-up in the permeate stream.

Separation factors for the four-column configuration were predicted from the sequential calculations of the model for a range of feed pressures and flow rates. The results plotted in Figure 9 show good agreement with the experimental values calculated from the data of Davis and Sandall.

All of these results lend confidence in the algebraic model. Students are able to quickly design alternative configurations and explore the potential performance of competing designs.

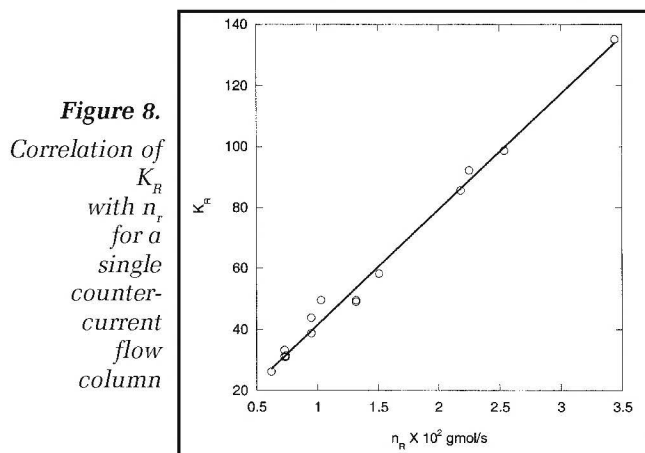


Figure 8. Correlation of K_R with n_r for a single countercurrent flow column

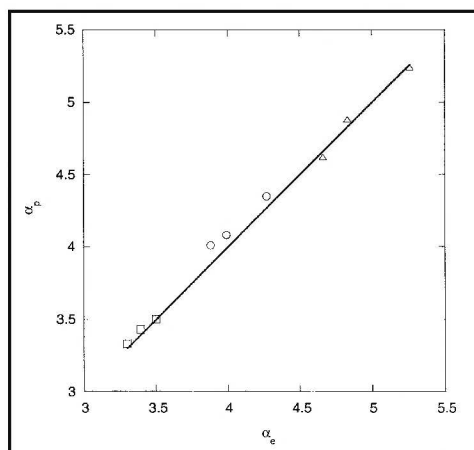


Figure 9. Comparison of predictions with experimental results for air separation in the four-column configuration: □=377 kPa, ○=515 kPa, △=653 kPa.

Membranes in ChE Education

For example, students usually start by comparing the performance of cocurrent and countercurrent flow. This leads to a design for one column operating in countercurrent flow with the same membrane surface area as the four columns. The single column design gives a predicted increase of 10% N_2 recovery when compared to the modular design. Students may use the models to predict a dimensionless membrane area, $1/K$, to recover a desired fraction of oxygen fed to the permeator. Other designs include four columns operating in parallel with countercurrent flow or four columns with the feed side in series and the permeate side in parallel.

The Mathcad files used in the analysis are available at <www.d.umn.edu/~rdavis/cee>

CONCLUSIONS

A membrane experiment for investigating gas separation has been in use for over ten years in the undergraduate laboratory at the University of California, Santa Barbara. A simple analysis method was presented that requires only the solution to a system of four algebraic equations. The simpler analysis is equally applicable to newer membrane configurations that introduce the high-pressure feed to the fiber bores in order to maintain better flow patterns in the membrane module. The experimental apparatus was designed to permit single- and four-column investigations of air separation. The single column was used to calibrate the models for binary gas separation. Comparing results for the four-column operation validated the calibrated model. Good model and experimental agreement lend confidence in the model and validate the model assumptions. Students are then able to use the model to develop competing designs for gas separation and optimize their designs for maximizing efficiency of separation. The advantages of the simpler approach are that students can readily set up and solve the model equations without complicated programming. Students are also able to explore alternative designs by building models and comparing the results.

NOMENCLATURE

A	membrane area, m^2
d	diameter, m
K	dimensionless membrane transport parameter
L	fiber length, m
n	molar flow rate, $gmol/s$
N	number of fibers in a bundle
p	permeate side pressure, kPa
P	feed side pressure, kPa
Q'	permeance, $gmol/(s \cdot kPa \cdot m^2)$
R	ideal gas constant, $kPa \cdot m^3/gmol \cdot K$
T	temperature, K
x	feed stream mole fraction of oxygen
y	permeate stream mole fraction of oxygen

z variable fiber length, m

Greek Symbols

α	experimental separation factor
Δ	transmembrane partial pressure, kPa
μ	viscosity, N-m/s
θ	cut of feed to permeate stream

Subscripts/Superscripts

c	closed end of fiber bore
e	experimental
f	fiber
F	feed
i	closed end of permeate stream
lm	log-mean result
m	membrane
N_2	nitrogen
O_2	oxygen
p	predicted
R	retentate
*	dimensionless or ideal parameter

REFERENCES

1. Pandey, P., and R.S. Chauhan, "Membranes for Gas Separation," *Prog. Polym. Sci.*, **26**(6), 853 (2001)
2. McCabe, W.L., J.C. Smith, and P. Harriott, *Unit Operations of Chemical Engineering*, 5th ed., McGraw-Hill, New York, NY (1993)
3. Geankoplis, C., *Transport Processes and Unit Operations*, 3rd ed., Prentice-Hall, Englewood Cliffs, NJ (1993)
4. Seader, J.D., and E.J. Henley, *Separation Process Principles*, John Wiley and Sons, New York, NY (1998)
5. Davis, R.A., and O.C. Sandall, "A Membrane Gas Separation Experiment for the Undergraduate Laboratory," *Chem. Eng. Ed.*, **25**(1), 10 (1991)
6. Walawender, W.P., and S.A. Stern, "Analysis of Membrane Separation Parameters. II: Counter-Current and Cocurrent Flow in a Single Permeation Stage," *Sep. Sci.*, **7**(5), 553 (1972)
7. Boucif, N., S. Majumdar, and K.K. Sirkar, "Series Solutions for a Gas Permeator with Countercurrent and Cocurrent Flow," *Ind. Eng. Chem. Fund.*, **23**, 470 (1984)
8. Thundiyil, M.J., and W.J. Koros, "Mathematical Modeling of Gas Separation Permeators: For Radial Crossflow, Countercurrent, and Cocurrent Hollow Fiber Membrane Modules," *J. Mem. Sci.*, **125**, 275 (1997)
9. Zolanz, R.R., and G.K. Fleming, "Design of Gas Permeation Systems," in *Membrane Handbook*, W.S. Ho and K.K. Sirkar, eds., Van Nostrand Reinhold, New York, NY, p. 66 (1992)
10. Bruining, W.J., "A General Description of Flows and Pressures in Hollow Fiber Membrane Modules," *Chem. Eng. Sci.*, **44**(6), 1441 (1989)
11. Federspiel, W.J., J.L. Williams, and B.G. Hattler, "Gas Flow Dynamics in Hollow-Fiber Membranes," *AIChE J.*, **42**(7), 2094 (1996)
12. Lim, S.P., X. Tan, and K. Li, "Gas/Vapour Separation Using Membranes: Effect of Pressure Drop in Lumen of Hollow Fibers," *Chem. Eng. Sci.*, **55**, 2641 (2000)
13. Mulder, M., *Basic Principles of Membrane Technology*, Kluwer Academic Publishers, Dordrecht, Netherlands (1991)
14. Chen, J.J.J., "Comments on Improvements on a Replacement for the Logarithmic Mean," *Chem. Eng. Sci.*, **42**(10), 2488 (1987)
15. Floudas, C.A., *Nonlinear and Mixed-Integer Optimization*, Oxford University Press, Oxford (1995)
16. Vladislavjevic, G.T., and M.V. Mitrovic, "Pressure Drops and Hydraulic Resistances in a Three-Phase Hollow Fiber Membrane Contactor with Frame Elements," *Chem. Eng. Proc.*, **40**, 3 (2001) □